

PAPER • OPEN ACCESS

Production of nanopowder of cerium (III) fluoride obtained by pulsed electron beam evaporation in vacuum

To cite this article: V G Ilves *et al* 2021 *J. Phys.: Conf. Ser.* **2064** 012085

View the [article online](#) for updates and enhancements.

You may also like

- [Energy Transfer in Er:CeF₃ Crystals](#)
Lei Ning, Feng Xi-qi, Hu Guan-qin et al.
- [Ionic-liquid-induced microfluidic reaction for water-soluble Ce_{1-x}Tb_xF₃ nanocrystal synthesis](#)
Nan Xie and Weiling Luan
- [The Free Energy of formation of CeF₃, and its Activity Coefficient in Cryolite.](#)
Ernest W. Dewing and Paul Desclaux



ECS
The
Electrochemical
Society
Advancing solid state &
electrochemical science & technology

DISCOVER
how sustainability
intersects with
electrochemistry & solid
state science research

Production of nanopowder of cerium (III) fluoride obtained by pulsed electron beam evaporation in vacuum

V G Ilves¹, S Y Sokovnin^{1,2} and M A Uimin^{2,3}

¹Institute of Electrophysics, 106 Amundsena St., Yekaterinburg, 620016, Russia

²Ural Federal University, 19 Mira St., Yekaterinburg, 620002, Russia

³M N Mikheev Institute of Metal Physics, 18 S. Kovalevskaya St., Yekaterinburg, 620108, Russia

E-mail: ilves@iep.uran.ru

Abstract. The method of pulsed electron beam evaporation in vacuum was first used to obtain CeF₃ nanopowder (NP). During NP production, a high evaporation rate of the target (~ 7 g/h) and a higher percentage of NP collection (> 72%) were observed, both for fluoride and the previously obtained CeO₂ oxide. It was found that the produced NP contains two crystalline phases: hexagonal CeF₃ (95 wt.%, coherent scattering region ≈ 8 nm and [Ce-O-F] or [Ce-F]). The magnetic susceptibility of CeF₃ nanoparticles (NPles) coincides with the susceptibility of micron particles, indicating the potential for using such NPles as a contrast agent for tomography. High specific surface area (CeO₂-270 m²/g, CeF₃ – 62 m²/g), large pore volume (0.35-0.11 cm³/g) allow the use of NPles as nanocontainers for drug delivery.

1. Introduction

Various methods for the production of nanofluorides are constantly proposed, promising for the creation of luminescent materials, catalysts, biomedical applications, etc. [1-3]. CeF₃ is one of the least stable rare earth trifluorides from pyrohydrolysis point of view [4, 5], and it also easily undergoes Ce(III) → Ce(IV) oxidation in the presence of oxygen. When the solid-state target is evaporated from the CeF₃ by pulsed electron beam evaporation (PEBE) under vacuum, the above-mentioned undesirable factors (pyrohydrolysis and oxidation) are eliminated.

The purpose of the work was to test the method of PEBE in vacuum [6] for the synthesis of trifluoride CeF₃ nanoparticles (NPles), to establish the main physicochemical characteristics of the obtained particles and to compare them with the corresponding characteristics of oxide NPles CeO₂.

2. Experimental section

2.1. Materials

Cerium(III) fluoride micron powder (CeF₃, 99.9%, free of water, China) was used for producing nanopowder (NP).

2.2. Characterization



The X-ray diffractogram was taken on the D8 DISCOVER diffractometer. Nitrogen adsorption and desorption isotherms at 77 K were obtained using Micromeritics TriStar 3000 V 6.03 A. Thermal analysis of the samples was carried out on thermoanalytic complex NETZSCH STA-409. Magnetic measurements were carried out using a Faraday balance at a RT.

3. Results and discussion

3.1. Synthesis of CeF_3 NP

The general scheme of the CeF_3 NP synthesis process from the raw material CeF_3 micron powder using the PEBE method in vacuum is shown in figure 1. The CeF_3 micron powder (figure 1 (a)) targets were pressed on a manual press in a titanium mold (figure 1 (b)). Target evaporation mode (figure 1 (c)): accelerating voltage 38 kV, beam current 0.3 A, pulse duration 100 μ s, repetition rate 100 Hz, evaporation time 45 min, amount of vaporized target material 4.4 g, NP collection (excluding losses) 3.1 g, NP collection percentage 72.3%. The resulting NP had very little adhesion to glass substrates. NP color is beige (figure 1 (d)).

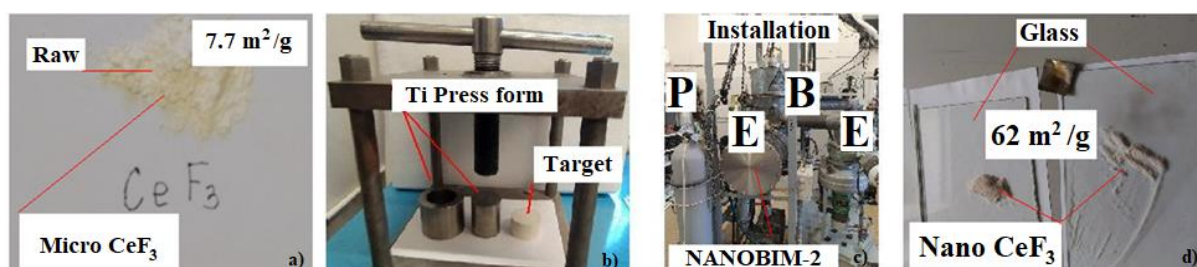


Figure 1. The general scheme of CeF_3 NP synthesis by PEBE in vacuum.

3.2. Structural analysis and morphology of synthesized CeF_3 NP

3.2.1. XRD analysis. Cerium trifluoride refers to the structural type of tysonite (LaF_3) which exists in two forms [7]. The low temperature phase l- CeF_3 has a trigonal structure. At the temperature $1107 \pm 25^\circ C$ [8], the l- CeF_3 phase turns into a more symmetrical high-temperature hexagonal phase h- CeF_3 (S. G. $P63/mmc$, $Z = 2$). In our work, the evaporation target was made of a single-phase powder consisting of a high-temperature h- CeF_3 phase with a hexagonal lattice, S.G.: $P63/mcm$ (193), with a coherent scattering region (CSR) size of 87 (3) nm, $a = 7.129$ (4) \AA , $c = 7.285$ (5) \AA , $\rho = 6.125$ (4) g/cm^3 . (PDF no. 01-089-1933, $a = 7.13$ \AA , $c = 7.29$ \AA , $\rho = 6.119$ g/cm^3). The CeF_3 NP X-ray diffraction pattern is shown in figure 2.

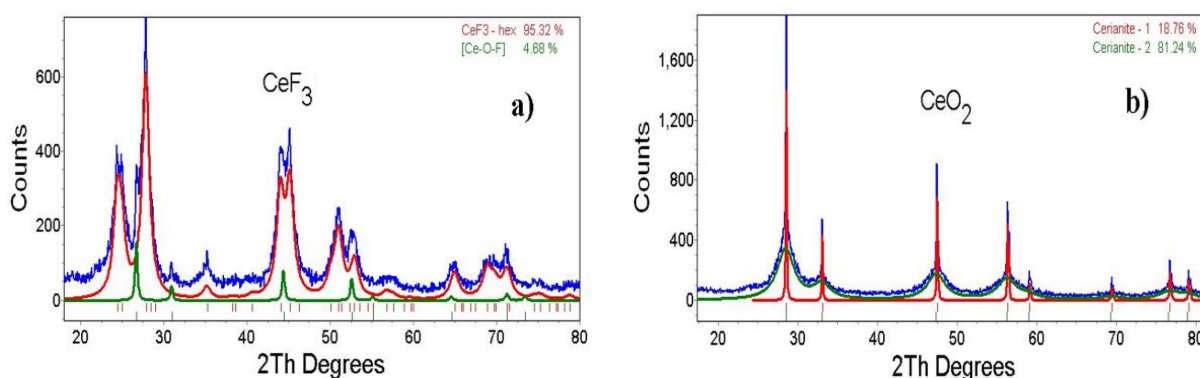


Figure 2. (a) X-ray diffraction pattern of CeF_3 NP prepared in vacuum; (b) X-ray diffraction pattern of CeO_2 NP prepared in vacuum.

The resulting NP contained two crystalline phases. The main phase (contents ≈ 95 wt.%) - CeF_3 , with hexagonal structure of S.G.: P63/mcm (193), with a size of CSR ≈ 8 nm and the lattice periods: $a = 7.12$ (2) \AA , $c = 7.29$ (2) \AA , $\rho = 6.15$ (4) g/cm^3 (PDF no. 01-089-1933, $a = 7.13$ \AA , $c = 7.29$ \AA , $\rho = 6.119$ g/cm^3). Possible impurity phase- [Ce-O-F] or [Ce-F], with a content of ≈ 5 wt.%. The diffractogram of the CeO_2 oxide NP is shown in figure 2 (b). The CeO_2 NP contained one phase: Cerianite CeO_2 with a cubic lattice S.G.: Fm-3m (225) (PDF no. 00-034-0394, $a = 5.4113$ \AA , $\rho = 7.215$ g/cm^3). When processing the results of XRD, the following model was used - CeO_2 consisted of two fractions: large-crystal and fine-dispersed (not amorphous). Cerianite - 1: content ≈ 19 wt.%, CSR = $120(\pm 10)$ nm, $a = 5,412(\pm 5)$ \AA , $\rho = 7,214(\pm 4)$ g/cm^3 ; Cerianite - 2, content ≈ 81 wt.%, CSR ≈ 3 nm, $a = 5,424(\pm 5)$ \AA , $\rho = 7.166(\pm 4)$ g/cm^3 . Thus, using the PEBE method, CeF_3 NP (~ 95 wt.%) with a CSR size ten times smaller than that of the original single-phase submicron powder CeF_3 was produced.

3.2.2. *Textural analysis.* Figure 3 shows isotherms of adsorption-desorption of trifluoride (micro and nano sizes) and cerium oxide and their pore size distribution.

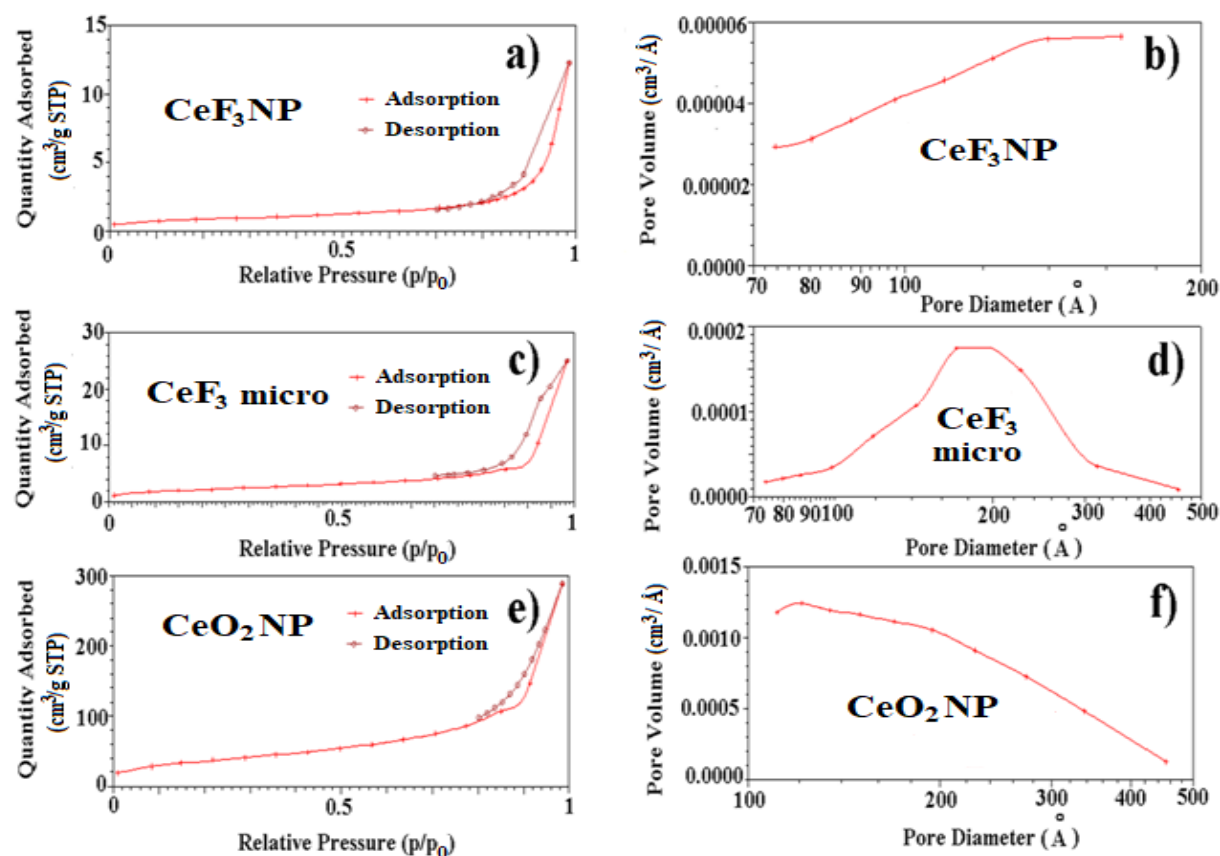


Figure 3. Nitrogen adsorption/desorption isotherm curves (a, c, e) and pore size distribution (b, d, f) of samples NPs CeF_3 , CeF_3 target and CeO_2 , respectively.

To establish the possible effect of the specific surface area (SSA) of CeF_3 nanopowder on their physicochemical properties, we tested samples of NP and S_{target} . The nitrogen isotherms of samples S0 and S_{target} in (figure 3 (a, c)) belong to the IV type with an H3 hysteresis loop according to IUPAC classification. The surface of the NP increased by 8 times compared to the SSA of the starting powder, the pore volume increased by three times, the pore size decreased from 21.5 nm to 12.3 nm. Improved textural parameters of CeF_3 nanopowder indicate its possible use as a nanocontainer for drug delivery,

as confirmed by recent studies [2]. The textural parameters of NP CeO₂ (table 1 and figure 3 (e, f)) are significantly higher than the corresponding parameters of cerium fluoride. The advantage of CeO₂ over CeF₃ relating to their use as a material for medicinal nanocontainers is obvious, however, CeF₃ has excellent paramagnetic, luminescent and X-ray characteristics compared to CeO₂ oxide and practically does not dissolve in water, which makes CeF₃ non-toxic [2] and a promising material for creating medicinal multimodal contrast agents based on it [9, 10].

Table 1. Results BJH (Barret-Joyner-Halenda) analysis.

Samples	SSA (m ² /g)	Pore Size (nm)	Pore Volume (cm ³ /g)
CeF ₃ target	7.2	21.5	0.04
NP CeF ₃	62.0	12.3	0.11
NP CeO ₂	129.3	23.8	0.35

3.3. Thermal analysis

The thermal stability of the obtained CeF₃ NP was determined using the synchronous differential scanning calorimetry and thermogravimetry (DSC-TG) method and mass spectral analysis. Figure 4 shows the DSC-TG synchronous heating/cooling curves and H₂O, CO₂ mass spectra of the sample CeF₃ NP in the temperature range 40-1400°C in argon atmosphere.

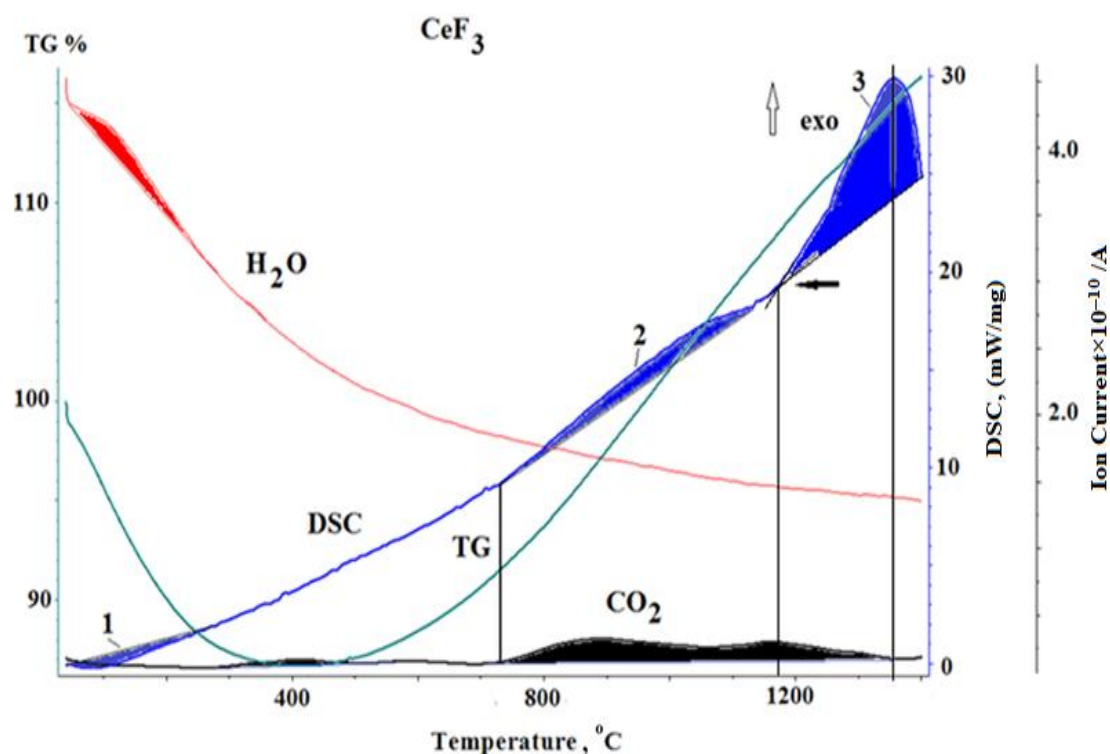


Figure 4. Synchronous heating curves DSC - TG and H₂O, CO₂ mass spectra of CeF₃ NP in the temperature range 40-1400°C in argon atmosphere.

Three thermal peaks are clearly visible on the DSC heating curve. Endothermic peak 1 in the range of 40-250°C was caused by evaporation of adsorbed water on the surface and in the pores of the NP. The weight loss of the sample continued only to the temperature of about 400°C. Up to the

temperature of 730°C, no thermal changes were observed on the DSC curve, however, on the TG curve, starting at the temperature 400°C, a constant increase in sample weight was observed, lasting up to the 1400°C temperature. Considering that the heating of the sample took place in an argon atmosphere, the increase in the mass of the sample can be explained by the physical adsorption of argon atoms in the pores of mesoporous CeF₃ NP. The thermal stability of the CeF₃ sample after heating to the temperature 730°C was possibly disturbed, as indicated simultaneously by an exothermic peak on the DSC curve (730-1170°C). It is most probable that the exothermic peak 2 could be caused by evaporation from the surface and from the pores of the sample impurity - cerium tricarbonat. A large exothermic peak 3 in the temperature range from 1170 to 1400°C (figure 4) is associated with the phase transformation of the metastable hexagonal phase CeF₃ into a more stable at high temperature x-CeF₃ phase, the structural type of which will be determined in the future. The adsorption of the inert gas Ar and the chemically inert gas N₂ on the mesoporous CeF₃ NP is of undeniable interest and requires further investigation.

3.4. Magnetic properties of CeF₃ NP

Figure 5 (a, b) shows the magnetization curves of fluoride and cerium oxide at room temperature.

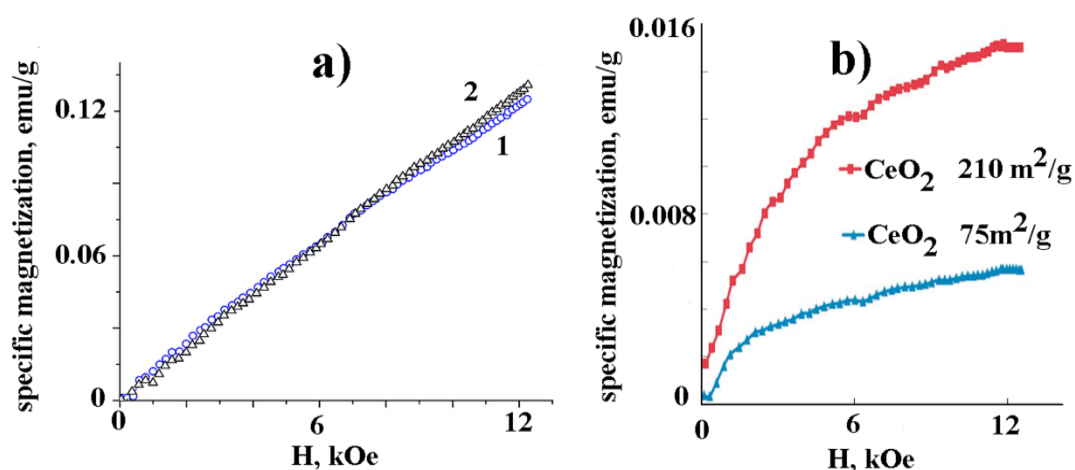


Figure 5. (a) Specific intensity of magnetization of CeF₃ NP prepared in vacuum: 1 - glass substrate; 2 - graphite substrate; (b) Specific intensity of magnetization of CeO₂ NPs prepared in vacuum CeO₂ [11].

Curves of magnetization of CeF₃ NP are linear functions of the field, and the susceptibility size determined by an inclination of curves corresponds to tabular value at the room temperature of $1.1 \times 10^{-6} \text{ cm}^3/\text{g}$, i.e. transition to a nanostate didn't affect magnetic behavior of CeF₃ in any way. In turn, the NP CeO₂ we obtained earlier by the PEBE method [11] showed a noticeable ferromagnetism (FM) difference (figure 5 (b)), which is consistent with the data on the magnetic behavior of CeO₂ NPles at RT given in the review [12] Note the recent work [13] in which a significant increase in FM at room temperature was observed in composite NPles of CeO₂/CeF₃. The saturation magnetization of CeO₂/CeF₃ composites (NPles size 100 nm) was half the magnetization of the initial LF CeO₂ (NPles size 30 nm). NPles of CeO₂/CeF₃ were synthesized by means of CeO₂ NP fluorination, therefore, presumably, NPles with the structure of CeF₃ were formed on CeO₂ NPles' surface. An increase in the saturation magnetization of CeO₂/CeF₃ NPles compared to the initial ones, as well as those annealed in vacuum and air, CeO₂ NPles, in [13] was linked to the interface of the fluorinated nanocomposites of CeO₂/CeF₃. Obviously, in order to obtain oxide-fluoride NPles, it is possible to use the reverse synthesis pathway to produce air annealing of paramagnetic CeF₃ NPles obtained by the PEBE method in vacuum at different temperatures, in order to obtain a FM controlled response in the NPles with

core-shell structure (core-CeF₃, shell CeO₂ (or Ce₂O₃), which should be formed during annealing. A similar study is expected in the near future.

4. Conclusion

The PEBE method was first used to produce nanoparticles CeF₃ under vacuum. There were produced the CeF₃ nanoparticles (95 wt.%, CSR ≈ 8 nm) with hexagonal structure. The textural parameters of mesoporous CeF₃ NP are significantly superior to the textural parameters of the micron mesoporous powder CeF₃. The paramagnetic properties of the obtained CeF₃ NP were comparable to the magnetic properties of the micron powder. High thermal stability, negligible small solubility in water makes the produced nanoparticles CeF₃ very attractive for their use in biomedical applications.

Acknowledgments

The reported study was funded by RFBR and GACR, project number 20-58-26002.

References

- [1] Chylli M, Loghina L, Kaderavkova A, Slang S, Rodriguez-Pereira J, Frumarova B and Vlcek M 2021 *Mater. Chem. Phys.* **260** 124161
- [2] Shcherbakov A B, Zholobak N M, Baranchikov A E, Ryabova A V and Ivanov V K 2015 *Mat. Sci. Eng. C-Mater* **50** 151–9
- [3] Fedorov P P, Luginina A A, Kuznetsov S V and Osiko V V 2011 *J. Fluorine Chem.* **132** 1012–39
- [4] Banks C V, Burke K E and O’Laudhlin J W 1958 *Anal. Chim. Acta* **19** 239–43
- [5] Mayakova M N, Voronov V V, Iskhakova L D, Kuznetsov S V and Fedorov P P 2016 *J. Fluorine Chem.* **187** 33–9
- [6] Sokovnin S Y and Ilves V G 2012 *Ferroelectrics* **436** 101–7
- [7] Sorokin N I, Karimov D N, Smirnov A N and Sobolev B P 2019 *Crystallogr. Rep.* **64** 105–9
- [8] Greis O and Cader M S R 1985 *Thermochim. Acta* **87** 145–50
- [9] Ma Z Y, Liu Y P, Bai L Y, An J, Zhang L, Xuan Y, Zhan X S and Zhao Y D 2012 *Dalton T.* **41** 4890
- [10] González-Mancebo D, Becerro A I, Rojas T C, Olivencia A, Corral A, Balcerzyk M, Cantelar E, Cussó F and Ocaña M 2018 *J. Colloid Interf. Sci.* **520** 134–44
- [11] Il’ves V G and Sokovnin S Y 2012 *Nanotechnologies in Russia* **7** 213–26
- [12] Ackland K and Coey J M D 2018 *Phys. Rep.* **746** 1–39
- [13] Morozov O A, Pavlov V V, Rakhmatullin R M, Semashko V V and Korableva S L 2018 *Phys. Status Solidi-R.* **12** 1800318